SCIENCE CHINA
Physics, Mechanics & Astronomy

•Article•

November 2021 Vol. 64 No. 11: 114612
https://doi.org/10.1007/s11433-021-1756-0

Odd elasticity realized by piezoelectric material with linear feedback

Wen Cheng, and Gengkai Hu*

School of Aerospace Engineering, Beijing Institute of Technology, Beijing 100081, China

Received May 15, 2021; accepted July 30, 2021; published online September 28, 2021

The systems exhibiting sustainable external energy exchange are abundant, e.g., biological organisms' reaction to external stimuli while maintaining a constant energy exchange with the surrounding. In a linear mechanical system exhibiting an external energy gain or release, the recently proposed odd elasticity theory can characterize the overall stress and strain response. However, realizing the required odd elasticity is still challenging. In this work, we discovered that the smart materials with designed feedbacks can achieve this odd elasticity, thereby providing a practical platform to analyze the phenomenon related to this novel elasticity theory. We also demonstrated this idea by designing a non-reciprocal Rayleigh wave via odd elasticity and the equivalent piezoelectricity with linear feedback. The underpinned electric energy scenario was also examined. Our work establishes a method to easily realize the materials with odd elastic behaviors and explore the rich phenomena related to non-Hermitian systems.

odd elasticity, piezoelectricity, feedback, Rayleigh wave, unidirectional invisibility

PACS number(s): 46.05.+b, 46.40.Cd, 77.65.–j, 77.65.Dq

Citation: W. Cheng, and G. Hu, Odd elasticity realized by piezoelectric material with linear feedback, Sci. China-Phys. Mech. Astron. **64**, 114612 (2021), https://doi.org/10.1007/s11433-021-1756-0

1 Introduction

The response of a linear elastic material to external small mechanical stimuli is characterized by Hooke's law, which describes a linear relationship between stress and strain as $\sigma_{ij} = C_{ijmn}\gamma_{mn}$, where C_{ijmn} is the material elastic tensor [1]. For passive materials without body couples, the elastic tensor has a minor ($C_{ijmn}= C_{jimn} = C_{ijnm}$) and major symmetry ($C_{ijmn}= C_{mnij}$). Therefore, in such systems, the time-reversal holds. This linear elastic model, also termed Green elasticity [2], is recognized as a potential tool for designing engineering structures [3].

However, the Green elastic model with the above linear Hooke's law is no longer applicable to the systems with sustainable external energy exchange, in which time-reversal symmetry is broken. Such systems are abundant, for example, in biological systems, such as cytoskeleton [4,5], liquid crystals [6], active membranes [7], and many others [8]. The common features of these systems are that the energy is supplied independently at the constituent level, which generates system movement in dissipating this energy; these systems are called active matter [9]. Their implications to engineering are also straightforward, for example, in bioinspired microrobots [10] and non-reciprocal wave propagation [11]. The systems with locally sustained external energy gain and release also form key ingredients of non-Hermitian physics [12].

To phenomenologically characterize the linear mechanical response of the active matter, a more general Cauchy elasticity theory could be explored to describe the external en-

*Corresponding author (email: hugeng@bit.edu.cn)

ergy exchange of the material [13]. Recently, Scheibner et al. [14] presented an alternative called odd elasticity theory. In this theory, the major symmetry of the elastic tensor is relaxed to consider the local external energy gain or release during loading. Odd elastic materials break the time-reversal symmetry; therefore, they can provide an ideal platform for demonstrating the unusual phenomena embodied in non-Hermitian systems [15,16]. In addition, the similar approaches are also extended to fluid [17] and flexural waves [18]. However, designing an odd elastic medium remains a future achievement. In this study, we use classical piezoelectric materials as a prototype and demonstrate that if a linear feedback control between the local strain and electric fields is provided, the piezoelectric material with such feedback control can be idealized as an odd elastic medium.

The remainder of this paper is organized as follows. In sect. 2, we demonstrate that the piezoelectric material with linear feedback can be considered as an odd elastic medium. In sect. 3, we investigate the bulk and edge waves in the homogeneous odd elastic medium to validate the proposed method, including a perfect matched layer and a non-reciprocal Rayleigh wave. These properties are validated using equivalent piezoelectric materials with the designed feedback. In sect. 4, the external energy exchange in an odd medium is revealed within a loading cycle, followed by some conclusions.

2 Connection between odd elasticity and piezoelectric materials with feedback

In this study, we consider a linear elastic material characterized by $\sigma_{ij} = K_{ijmn}\gamma_{mn}$, where σ_{ij} and γ_{mn} are the stress and strain tensors, respectively. The fourth-order elastic tensor K_{ijmn} can be decomposed into a symmetric part C^{e}_{ijmn} ($C^{e}_{ijmn} = C^{e}_{mnij}$) and an antisymmetric part C^{o}_{ijmn} $\left(C^{o}_{ijmn} = -C^{o}_{mnij}\right)$ as:

$$K_{ijmn} = C^{e}_{ijmn} + C^{o}_{ijmn}. \tag{1}$$

A passive linear material obeys the Maxwell-Betti reciprocity principle, implying that the elastic work is conserved and should be zero in one static deformation cycle. This constrains the elastic tensor to have the major symmetry, i.e., $K_{ijmn} = K_{mnij}$, while the antisymmetric part vanishes. Here, $K_{ijmn} = C^{e}_{ijmn}$, which is widely used in the Green elastic material. However, for active linear materials, the antisymmetric part in eq. (1) is necessary to characterize the non-conservative energy in the considered system, and the elastic tensor has no major symmetry $K_{ijmn} \neq K_{mnij}$. The elastic medium with this feature is called "odd elasticity", which was first presented in viscoelastic systems [19] and recently extended to the non-Hermitian elastic system [14]. Since an odd elastic material breaks the time-reversal symmetry, it can neither be made by passive materials nor by classical smart materials with no feedback control. Among smart materials, piezoelectric materials are widely used in engineering applications, and the general piezoelectric constitutive relation can be written as follows:

$$\begin{aligned} &\sigma_{ij} = C^{0e}_{ijmn}\gamma_{mn} - e_{kij}E_k, \\ &D_k = e_{kij}\gamma_{ij} + \varepsilon_{kl}E_l, \end{aligned} \tag{2}$$

where D_k and E_k are, respectively, the electric displacement and electric field strength; e_{kij} and ε_{ij} denote the piezoelectric modulus and dielectric permittivity, respectively. In piezoelectric materials, the elastic tensor C^{0e}_{ijmn} has a major symmetry.

Here, we consider the inverse piezoelectric effect, i.e., the electric field induces deformations. If we can provide a linear feedback control between the local strain and electric field such that $E_k = \zeta_{kmn}\gamma_{mn}$ and focus only on the mechanical part, we get the equation:

$$\sigma_{ij} = C^{0e}_{ijmn}\gamma_{mn} - e_{kij}\zeta_{kmn}\gamma_{mn} = K_{ijmn}\gamma_{mn}, \tag{3}$$

where $K_{ijmn} = C^{0e}_{ijmn} - e_{kij}\zeta_{kmn}$. Evidently, K_{ijmn} loses its major symmetry as required by odd elasticity. Comparing with eq. (1), we get

$$\begin{aligned} &C^{e}_{ijmn} = K_{ijmn} - \left(e_{kij}\zeta_{kmn} + e_{kji}\zeta_{knm}\right)/2, \\ &C^{o}_{ijmn} = -\left(e_{kij}\zeta_{kmn} - e_{kji}\zeta_{knm}\right)/2. \end{aligned} \tag{4}$$

The external electric field introduces the odd part of the stiffness tensor and modifies the elastic modulus tensor C^{e}_{ijmn} of the system. Figure 1 depicts the principle of designing an odd elastic medium. To achieve an odd homogeneous elastic medium, we consider a piezoelectric material and divide it into small elements; each element comprises a sensor and an actuator, as depicted in Figure 1(c). While the material is deformed, the sensor delivers a signal, and the actuator creates a strain with a proper transfer function. If each element is small enough and works independently, the mechanical response of the whole system can be characterized by an odd elastic medium. In practice, we can use piezoelectric composites instead of the pure piezoelectric material; the underlying principle remains the same.

From the energy point of view, the variation of the internal energy comes from the mechanical and electrical parts. It can be written as:

$$\mathrm{d}W = \sigma_{mn}\mathrm{d}\gamma_{mn} + D_k\mathrm{d}E_k. \tag{5}$$

If we consider a linear feedback with the electric field and local strain, the variation of the internal energy is further written as:

$$\mathrm{d}W = \sigma_{mn}\mathrm{d}\gamma_{mn} + D_k\zeta_{kmn}\mathrm{d}\gamma_{mn} = \tilde{\sigma}_{mn}\mathrm{d}\gamma_{mn}, \tag{6}$$

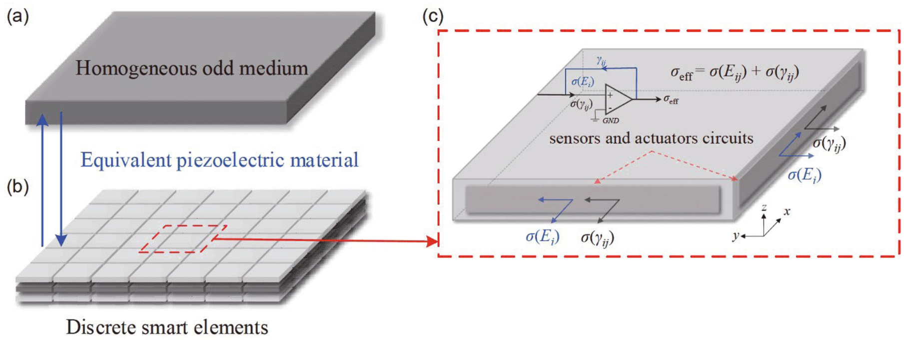

Figure 1 (Color online) Schematic of the principle to realize an odd elasticity by piezoelectric material with feedback. (a) Homogeneous odd elastic medium; (b) equivalent piezoelectric material with feedback control; (c) the scheme of feedback control.

here the effective stress $\tilde{\sigma}_{mn}$ consists of two parts: one from the mechanical strain and the other from the electric field due to the feedback coupling. From eq. (6), the odd elasticity can be explained as follows: if the coupling between the two types of independent variables (γ_{mn} and E_k) for a linear piezoelectric material is established via a feedback mechanism, the total energy can be expressed in terms of reduced independent variables (here γ_{mn}). This results in a new effective elastic tensor without a major symmetry, which accounts for the electric energy apart from the mechanical energy.

In other words, for a piezoelectric material with a linear feedback mechanism, its mechanical response can be characterized by an odd homogeneous elastic material. The extra energy gain or release besides the usual mechanical energy is provided by the electric energy. Using the same rationale, we can also choose the reduced independent variable as E_k and define an odd piezoelectric material; here, the extra external energy release or gain is provided by the mechanical energy.

The above concept can be extended to other smart materials. In what follows, we illustrate this concept using two examples: the impedance matched design and non-reciprocal Rayleigh wave.

3 Bulk and edge waves in an odd elastic medium

3.1 A brief introduction to odd elasticity

In this subsection, we outline some basic ingredients of a two-dimensional (2D) isotropic odd elastic medium proposed by Scheibner et al. [14]. To gain a better understanding of odd elastic parameters, the deformations are defined by s_α (α = 0, 1, 2, 3) as follows:

$$\begin{aligned} s_0 &= u_{1,1}+u_{2,2},\\ s_1 &= u_{2,1}-u_{1,2},\\ s_2 &= u_{1,1}-u_{2,2},\\ s_3 &= u_{1,2}+u_{2,1}, \end{aligned} \tag{7}$$

where the above deformations s_0 and s_1 represent the dilation and rotation, respectively (anticlockwise is defined positive), and s_2 and s_3 denote two types of shear strain. Similarly, we can also define the corresponding stress t_α, representing separately the pressure, torque, and two types of shear stress. For a 2D isotropic odd elastic medium, we can write the relationship between the strain and stress defined previously as:

$$\begin{bmatrix} t_0\\ t_1\\ t_2\\ t_3 \end{bmatrix} = 2\begin{bmatrix} \kappa & & & \\ A & & & \\ & & \mu & K_0\\ & & -K_0 & \mu \end{bmatrix}\begin{bmatrix} s_0\\ s_1\\ s_2\\ s_3 \end{bmatrix}. \tag{8}$$

Besides the two traditional parameters, κ (bulk modulus) and μ (shear modulus), the 2D isotropic odd elastic medium also has two additional coupling parameters A and K_0, representing the coupling between rotation and dilation, shear$_1$ and shear$_2$, respectively, as illustrated by Figure 2.

In a linear elastic material, torque is decoupled through rotation due to the conservation of the angular momentum. This coupling may appear by a careful micro-structural design [20] or by imposing additional external moments [21]. However, these methods are not treated in this paper. For simplicity, we will focus on the K_0-type (only shear coupling, A = 0 and $K_0 \neq 0$) odd elastic medium. The constitutive relation in eq. (8) can be written in a traditional type (Voigt notation):

$$\begin{bmatrix} \sigma_{11}\\ \sigma_{22}\\ \sigma_{12} \end{bmatrix} = \begin{bmatrix} \kappa+\mu & \kappa-\mu & K_0\\ \kappa-\mu & \kappa+\mu & -K_0\\ -K_0 & K_0 & \mu \end{bmatrix}\begin{bmatrix} \gamma_{11}\\ \gamma_{22}\\ 2\gamma_{12} \end{bmatrix}, \tag{9}$$

where K_0 is a material constant introduced to characterize the external energy exchange. It contains information on the amplitude of this exchange and its variation with time during the mechanical loading; therefore, it is generally a complex value. It should also be emphasized that the odd elasticity is fundamentally different from an anisotropic linear elastic material. To realize the odd elastic material defined by eq. (9), we consider a piezoelectric medium with the following classical constitutive relation:

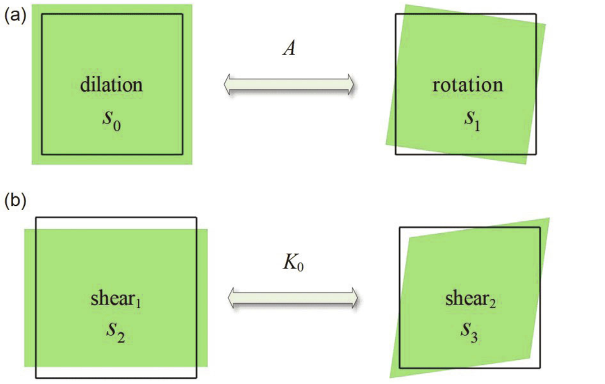

Figure 2 (Color online) Classification of 2D strains and their coupling. (a) Coupling between dilation and rotation; (b) coupling between two shear modes. The box with solid lines represents the original geometry, and the green-colored region represents the deformed shape.

$$\begin{bmatrix}\sigma_{11}\\ \sigma_{22}\\ \sigma_{12}\end{bmatrix}=\begin{bmatrix}\kappa+\mu & \kappa-\mu & 0\\ \kappa-\mu & \kappa+\mu & 0\\ 0 & 0 & \mu\end{bmatrix}\begin{bmatrix}\gamma_{11}\\ \gamma_{22}\\ 2\gamma_{12}\end{bmatrix}-\begin{bmatrix}e_{111} & 0\\ e_{221} & 0\\ 0 & e_{122}\end{bmatrix}\begin{bmatrix}E_x\\ E_y\end{bmatrix}, \tag{10}$$

where the mechanical part is isotropic with bulk modulus κ and shear modulus μ, respectively. Following the idea explained in sect. 2, we may set $e_{221} = -e_{111}$ and choose the feedback tensor as:

$$\begin{bmatrix}E_x\\ E_y\end{bmatrix}=\begin{bmatrix}0 & 0 & -K_0/e_{111}\\ K_0/e_{122} & -K_0/e_{122} & 0\end{bmatrix}\begin{bmatrix}\gamma_{11}\\ \gamma_{22}\\ 2\gamma_{12}\end{bmatrix}. \tag{11}$$

Substituting eq. (11) into eq. (10) and eliminating the electrical degree of freedom, we get the same form of the stress and strain relation as that for the odd homogeneous elasticity described by eq. (9).

In general, an odd elastic medium cannot be impedance-matched with any linear elastic material; there could be significant scattering at the interface formed between an odd elastic medium and a linear Green elastic material. However, based on the concept introduced in sect. 2, the odd elastic medium can be impedance-matched with a piezoelectric material if a proper feedback mechanism between the local strain and the electric field is provided. To verify this remark and prove the concept advanced in sect. 2, we analyze a shear wave propagation in a semi-infinite homogeneous odd elastic medium joined separately with a semi-infinite homogeneous linear elastic material and the equivalent piezoelectric medium with a proper feedback mechanism. In the computation, the odd elasticity is realized by modifying the weak form of the governing equation, and the perfect matched layer (PML) for the odd elasticity is constructed following the asymmetric transformation [22,23]. Both the odd elasticity and the equivalent piezoelectricity are conducted with the commercially available COMSOL Multiphysics.

Figure 3(a) depicts the curl of the displacement fields in the frequency domain when a shear wave travels from the odd elastic medium to the linear elastic material resulting in a significant scattering due to the impedance mismatch. However, a perfect transmission is observed at the interface formed by the odd elastic medium and its equivalent piezoelectric material, as shown in Figure 3(b).

Since odd elastic materials favor external energy exchange, they can break the time-reversal symmetry. In the next section, we explore some unique wave characteristics in these types of elastic materials, including a non-reciprocal Rayleigh wave.

3.2 Non-reciprocal Rayleigh wave

Rayleigh wave is a type of surface wave propagating along the free surface of a semi-infinite elastic medium and decaying in-depth [24]. The control of Rayleigh waves plays an important role in engineering, e.g., alleviating seismic waves [25] and non-destructive structure health monitoring [26]. For a linear passive medium, Rayleigh waves always have two symmetric velocities propagating in opposite directions along a free surface because of the requirement of reciprocity. Recently, it has been proved that a non-reciprocal surface wave can be achieved with a time-varying material [27,28] and a gyroscopic medium [29]. For a gyroscopic 2D homogeneous elastic medium, Zhou's group [11] extended the Stroh formalism [30] to chiral density and demonstrated the possibility of having a non-reciprocal Rayleigh wave in

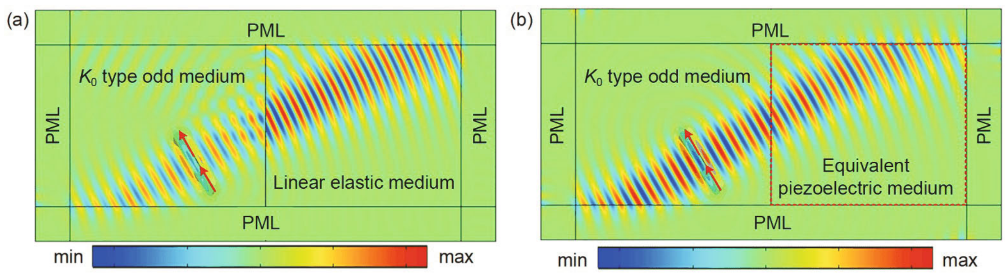

Figure 3 (Color online) Shear wave propagates in a semi-infinite odd elastic medium joined by (a) linear elastic material and (b) the equivalent piezoelectric medium. We set classical elastic parameters as $\kappa = 53.8$ [GPa], $\mu = 25.9$ [GPa], and $\rho = 2700$ [kg/m^3]. They are the same for the three examined media, the odd parameter $K_0 = 0.3\kappa$, the piezoelectric parameters $e_{221} = -e_{111} = 6.1$ [Pa m/V], and $e_{122} = 15.7$ [Pa m/V]. The excitation frequency is 30 kHz.

this medium. Here we extended the Stroh formalism to an odd elastic medium and demonstrated the appearance of a non-reciprocal Rayleigh wave in such a medium.

For simplicity, we also consider a 2D semi-infinite K_0-type odd elastic medium with a free surface characterized by its unit normal vector $\mathbf{e}_y$ and unit tangential vector $\mathbf{e}_x$, as depicted in Figure 4. The governing equation can be written as:

$$\nabla \cdot [\mathbf{K} : \nabla \mathbf{u}] = \rho \ddot{\mathbf{u}}, \tag{12}$$

where $\mathbf{K}$ denotes the elastic tensor of the odd elastic medium given by eq. (9), $\mathbf{u}$ represents the displacement, and the two dots stand for a second-order time derivative. The displacement u_k is assumed to be

$$u_k = U_k \mathrm{e}^{-\mathrm{i}p(x+qy-vt)}, \tag{13}$$

where v denotes the surface wave speed (phase velocity), U_k the amplitude of the displacement u_k, p the wave vector of the Rayleigh wave, and q characterizes the decaying wave in depth. Substituting this expression into the governing equation yields

$$\left[K_{\mathrm{i}1k1} + q(K_{\mathrm{i}1k2} + K_{\mathrm{i}2k1}) + q^2 K_{\mathrm{i}2k2} - \rho\delta_{\mathrm{i}k} v^2\right] U_k = 0. \tag{14}$$

In general, we need to combine eq. (14) with the boundary condition ($T_i = \sigma_{ij} n_j = 0$) to determine the surface wave speed; this leads to a quadratic eigenvalue problem with q. However, Stroh's formalism can largely reduce it to a linear equation. For that, we define a generalized vector:

$$\boldsymbol{\varphi} = \left[U_1 \quad U_2 \quad -T_1/\mathrm{i}p \quad -T_2/\mathrm{i}p\right]^{\mathrm{T}}. \tag{15}$$

Together with the governing equation, we obtain a linear eigenvalue problem with q, as given by eq. (16), the detailed derivation is provided in the Appendix.

$$\begin{bmatrix} \frac{2K_0\kappa}{K_0^2+\mu(\kappa+\mu)} & -1 & \frac{\kappa+\mu}{K_0^2+\mu(\kappa+\mu)} & -\frac{K_0}{K_0^2+\mu(\kappa+\mu)} \\ 1-\frac{2\kappa\mu}{K_0^2+\mu(\kappa+\mu)} & 0 & \frac{K_0}{K_0^2+\mu(\kappa+\mu)} & \frac{\mu}{K_0^2+\mu(\kappa+\mu)} \\ -\frac{4\kappa\left(K_0^2+\mu^2\right)}{K_0^2+\mu(\kappa+\mu)}+\rho v^2 & 0 & -\frac{2K_0\kappa}{K_0^2+\mu(\kappa+\mu)} & 1-\frac{2\kappa\mu}{K_0^2+\mu(\kappa+\mu)} \\ 0 & v^2\rho & -1 & 0 \end{bmatrix} \times \begin{bmatrix} \varphi_1 \\ \varphi_2 \\ \varphi_3 \\ \varphi_4 \end{bmatrix} = q \begin{bmatrix} \varphi_1 \\ \varphi_2 \\ \varphi_3 \\ \varphi_4 \end{bmatrix}. \tag{16}$$

In the frequency domain, the imaginary part of K_0 represents the phase difference between the mechanical loading and external energy exchange achieved by adjusting the cadence of the injected energy. We found that only if $\arg(K_0) = \pm\pi/2$ ($\mathrm{Re}[K_0] = 0$), the wave speed has two real solutions; otherwise, they must be complex. This point is emphasized at the end of this section. Presently, we only consider the case where $\arg(K_0) = \pm\pi/2$. Eq. (16) presents the Stroh's formalism to determine the surface wave of an odd elastic surface; two propagation speeds $v_\pm$ (in the positive and negative directions) are obtained by solving eq. (a10) (see the Appendix). In traditional Green elastic materials, the two speeds are equal; however, in a non-conservative system characterized by the odd elasticity, both speeds may be different; one may be zero leading to a non-reciprocal Rayleigh wave or even an unidirectional propagation. In addition, solved speed below a cutoff velocity v_c needs to be maintained [31,32], for the considered odd elastic medium, written as:

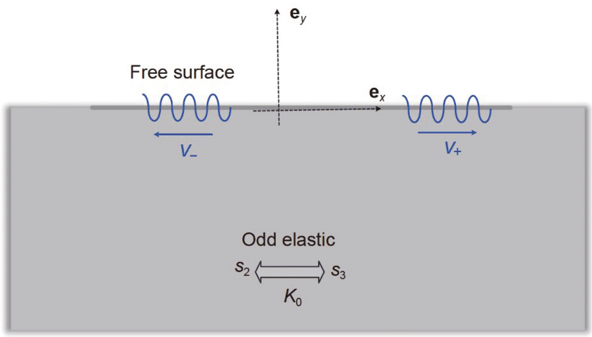

Figure 4 (Color online) Scheme of Rayleigh wave with velocity v_+ and v_- in two opposite directions along a free surface, the semi-infinite odd elastic medium has shear coupling coefficient K_0.

$$v_\mathrm{c}^2 = \frac{(\kappa+2\mu) - \sqrt{\left(\kappa^2 - 4K_0^2\right)}}{2\rho}. \tag{17}$$

Figure 5(a) depicts the ratio of the two surface wave speeds $|v_+/v_-|$ represented by color as a function of two dimensionless material parameters $\alpha = \mathrm{Im}[K_0]/\kappa$ and $\beta = \mu/\kappa$. Three distinct regions are observed. First, the black line where $\alpha = 0$ suggests the reciprocal Rayleigh wave propagations with two equal speeds but in opposite directions. Second, the colored region is separated by the reciprocity line and the boundary defined by the cutoff velocity. In this region, two different surface wave speeds are found, indicating a non-reciprocal Rayleigh wave propagation. Third, the region is enclosed by the boundary of the cutoff velocity and horizontal axis. Since one wave is prohibited in this region due to the speed solved by Stroh equation in excess of the cutoff velocity, only a unidirectional Rayleigh wave is allowed. To be more specific, the Rayleigh wave propagates only in the negative direction for $\alpha < 0$ and in the positive direction for $\alpha > 0$. The sign of the odd parameter K_0 determines the direction of the edge state.

To realize the non-reciprocal Rayleigh wave predicted by the homogeneous odd elastic material, we explore its equivalent piezoelectric counterpart explained previously. To mimic the complex odd elastic parameter, we modify the feedback tensor as a pure imaginary number in the frequency domain. Figure 6 shows Rayleigh waves realized by the equivalent piezoelectric material with the designed feedback, which mimics exactly the cases shown in Figure 5(b) and (c).

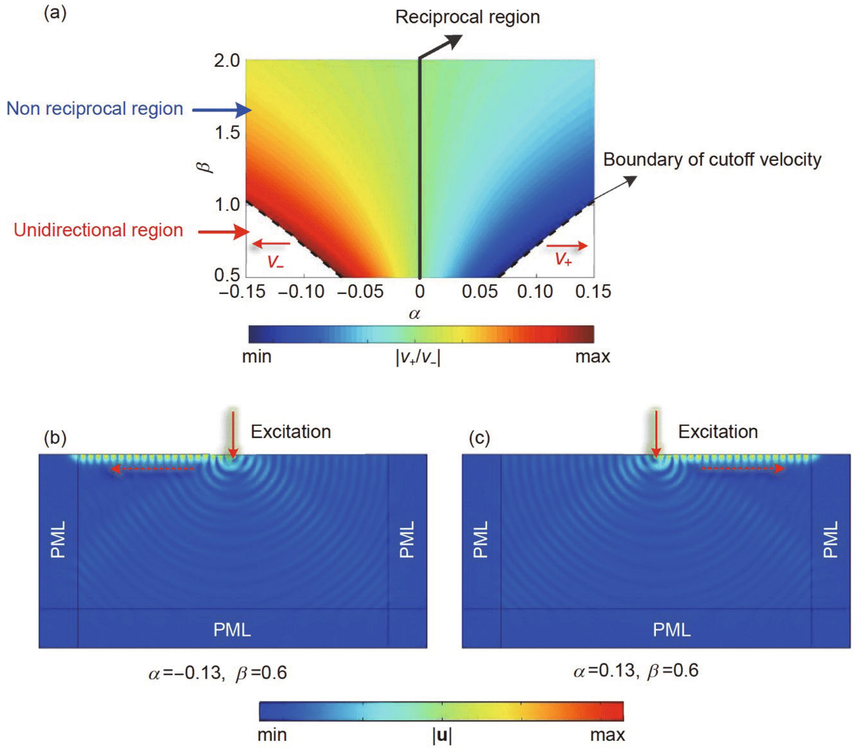

Figure 5 (Color online) Rayleigh wave in K_0-Type odd elastic medium. (a) Ratio of surface speeds $|v_+/v_-|$ as function of two dimensionless material parameters. Three regions are observed, reciprocal, non-reciprocal, and unidirectional Rayleigh waves, respectively. Simulation results for unidirectional surface wave propagations for (b) α=−0.13 and (c) α=0.13. We set the other material parameters as κ = 53.8 GPa, ρ = 2700 kg/m^3.

For comparison, the reciprocal Rayleigh wave is also shown in Figure 6(b) without feedback control. In Figure 6(d) and (e), we additionally provide the underpinned electric field pattern necessary for the piezoelectric material to produce the same phenomena as predicted by the homogeneous odd elastic material.

So far, we have analyzed the case where the odd elastic material parameter satisfies the condition $\arg(K_0) = \pm\pi/2$. For the case where $\arg(K_0) \neq \pi/2$, e.g., $K_0 \in R$, the solution of eq. (14) yields a complex value for v. Here, the surface wave vector **p** is also complex, its real part characterizes a traveling wave, and its imaginary part describes a decaying or amplifying edge state. This is a striking feature observed in non-Hermitian systems, referred to as unidirectional invisibility [33], i.e., the power of wave increases in one direction and decreases in the opposite. Figure 7 shows schematically the different edge modes for the value of $\arg(K_0)$, e.g., the evanescent mode for $\arg(K_0)$=0, travelling mode for $\arg(K_0)$=±π/2, and evanescent or power growth mode for $\arg(K_0)$=0, π. The cases indicated by Figure 7(a) and (c) generally appear in the opposite directions along a free surface, as shown more clearly in Figure 7(d) and (e) and calculated with the homogeneous odd elastic material with the same loading as discussed previously. By adjusting the feedback phase between the local strain and the electric field, the same phenomenon can also be achieved using the equivalent piezoelectric material.

4 Energy scenario of odd elastic materials

As discussed in the previous section, the odd elastic materials can regulate the external energy exchange during deformations. It is, thus, interesting to examine this energy flow necessary to maintain the odd elastic medium, on which the interesting phenomena discussed in sect. 3 are based.

Considering a square element of a 2D K_0-type odd elastic medium (K_0/κ=0.1), the deformation of such element is decomposed into the basis strain s_2 and s_3 in the space of shear strains (for example eq. (7)), as shown in Figure 8(a). We consider one cycle linear strain loading s=s_2+s_3. Since the total strain is composed of s_2 and s_3, two loading paths can be envisaged: path 1, marked by the red circle in Figure 8(a) has the loading sequence s=0→s_2→s_2+s_3→s_3→0 (Figure 8(b) forward direction); path 2, denoted by the blue circle in Figure 8(a), has the loading sequence s=0→s_3→s_2+s_3→s_2→0 (Figure 8(b) backward direction). The variation of the strain energy during each loading cycle can be written as:

$$w_{\text{odd}} = \frac{1}{2} \oint t_{\alpha} \mathrm{d}s_{\alpha}. \quad (18)$$

For the equivalent piezoelectric material, the increment of

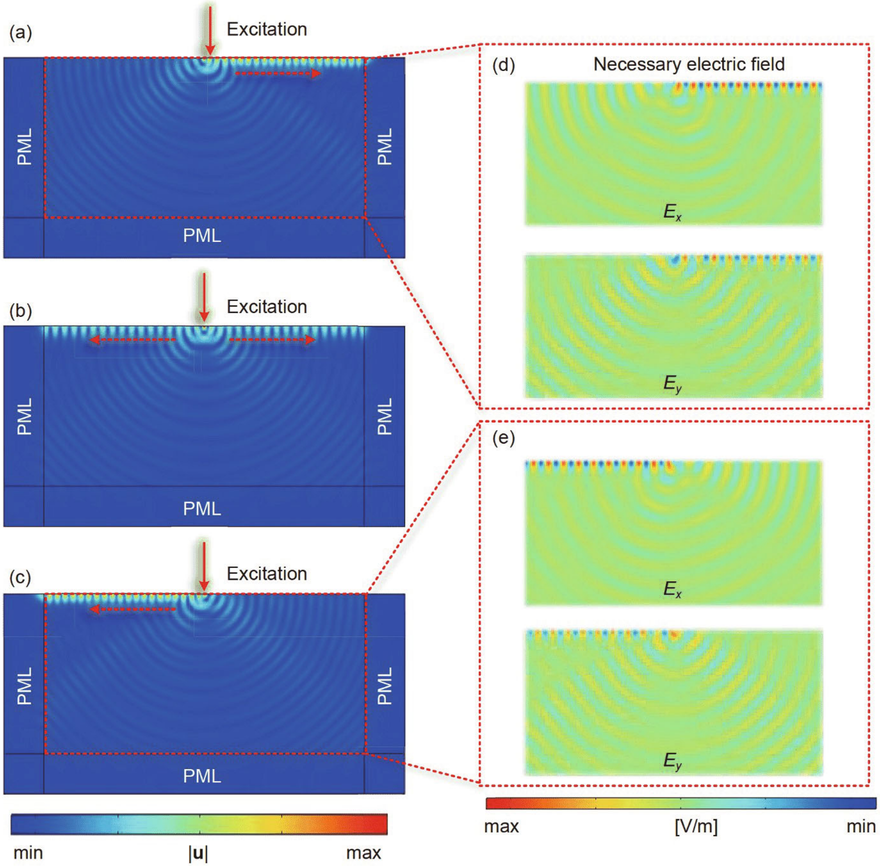

Figure 6 (Color online) Rayleigh wave achieved with equivalent piezoelectric material. Unidirectional Rayleigh wave rightward (a) and leftward (c). Necessary electric field intensity E_x and E_y during the feedback rightward case (d), leftward case (e), and reciprocal Rayleigh wave without feedback control (b). We set material parameters as κ=53.8 GPa, μ=32.3 GPa, and ρ = 2700 kg/m^3.

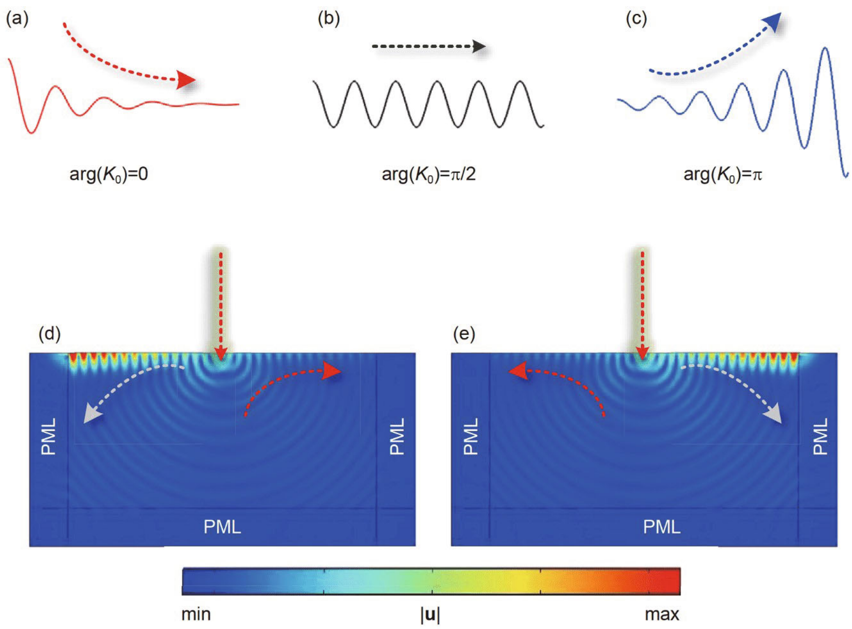

Figure 7 (Color online) Different edge modes based on the phase of K_0. (a) Evanescent mode, (b) traveling mode, and (c) power growth mode. (d) and (e) show the unidirectional invisibility in two opposite directions in an odd elastic media (left: K_0/κ=0.06 and right: K_0/κ=−0.06).

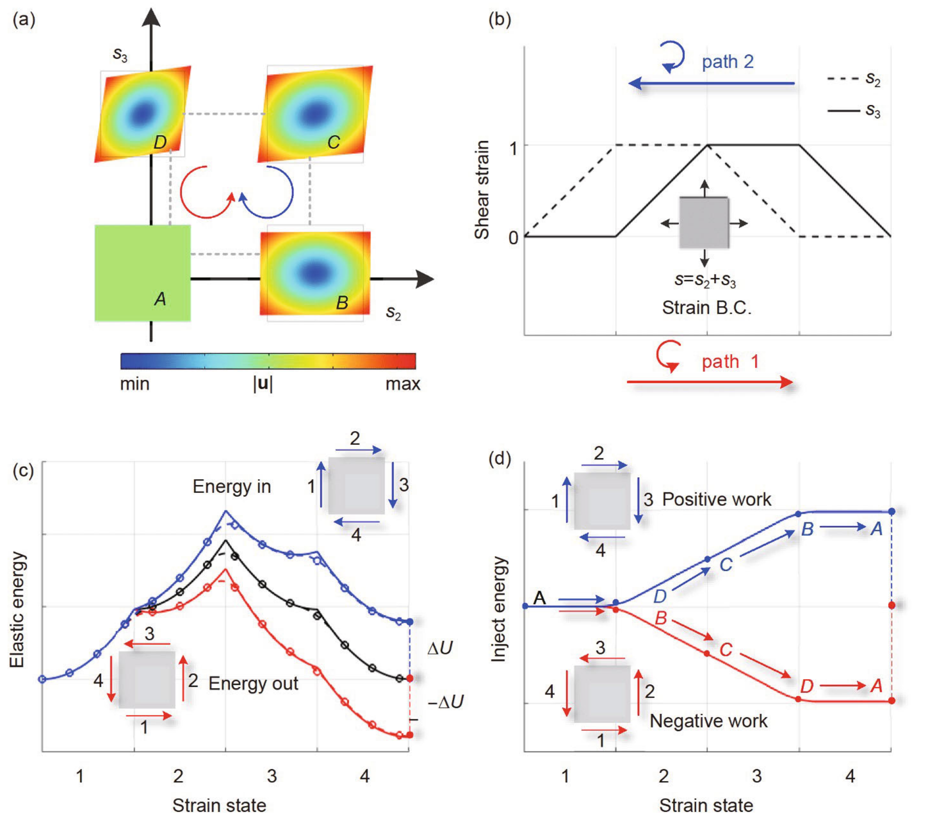

Figure 8 (Color online) Energy variations of an odd elastic medium and the equivalent piezoelectric material during one strain loading cycle. (a) An odd elastic material element is deformed in one strain loading cycle in strain space. The anticlockwise loading sequence is defined as path 1 (red circle), and the clockwise loading sequence is defined as path 2 (blue circle). (b) The strain loading sequence for path 1 and path 2, respectively. (c) Analytic results (solid lines) and simulation results (dash lines with circle) of the energy variation in one loading cycle. (d) Energy gain (blue line) or release (red line) via coupling energy during one loading cycle.

the apparent strain energy is given by $dw_{\text{piezo}}=\sigma_{ij}d\gamma_{ij}$, including some part of the electric energy due to the feedback eq. (6). The incremental coupling energy is defined by $dw_{\text{couple}}=-e_{kij}E_k d\gamma_{ij}$. With such a definition, we can examine the strain energy scenario of the system in one deformation cycle. The analytic result (solid lines) of the homogeneous odd elastic medium and simulation result (dash lines with circle) of the equivalent piezoelectric material are shown respectively in Figure 8(c). The red and blue line represent the energy variations along the path 1 and path 2, respectively. As seen, both the odd elastic and the equivalent piezoelectric materials do not conserve energy. Moreover, they also depend on the loading path because after a loading cycle the apparent strain energies do not return to zero. For comparison, the black line in the middle represents a classical isotropic medium with the same κ and μ as the odd elastic medium. The strain energy returns to zero after a deformation cycle as expected.

To illustrate the modulated external energy flow, we calculated the variations of the coupled energy during one deformation cycle along different loading paths, shown in Figure 8(d). The difference between the coupled energy variation lies in the antisymmetric coupling between two shear deformations. The s_3 strain leads to a positive stress t_2, whereas the s_2 strain leads to a negative stress t_3 as shown below:

$$\begin{bmatrix} t_2 \\ t_3 \end{bmatrix} = 2\begin{bmatrix} \mu & K_0 \\ -K_0 & \mu \end{bmatrix}\begin{bmatrix} s_2 \\ s_3 \end{bmatrix}. \tag{19}$$

Figure 8(d) demonstrates that the energy is pumped out for the loading path 1 (red line). To explain this effect, we consider the work done by t_2 in the deformation cycle firstly. During the loading process $B\rightarrow C$, no work is done by t_2 since s_2 is constant, as seen in Figure 8(a); however, t_2 increases because of the positive coupling K_0. Compared with the energy gain in the process $A\rightarrow B$, the energy released in the process $C\rightarrow D$ is greater than the energy gain due to the increase of t_2 in the loading process $B\rightarrow C$. This additional energy release is provided by the negative work done by the electric field in the loading process $C\rightarrow D$. A similar mechanism holds for the negative work done by t_3. However, if there is a phase difference between the energy exchange and mechanical loading, which equals $\arg(K_0)=\pm\pi/2$, the energy gain or release is balanced, based on the above analysis. Any system with this feature is called a PT-symmetry (pseudo-Hermitian) system [34]. It is also the physical mechanism governing the existence of a stable non-reciprocal surface wave, as discussed in the previous section.

The additional electric field only affects the odd material parameters, but the elastic modulus remains unchanged in this case. While the feedback is introduced in a system, the feedback can be decomposed into even parts and odd parts. In a static deformation cycle, the equivalent medium releases or gains energy through the odd part, and the even part only affects the energy amplitude. Finally, since both the odd and Cauchy elasticities can characterize the energy injected or released during a mechanical loading cycle, the odd elasticity may be a special category of Cauchy elasticity. More studies to prove this observation are necessary and underway.

5 Conclusions

We demonstrated that an odd elastic medium could be mimicked using a piezoelectric material with carefully designed linear feedback between the local strain and electric field. In other words, for a piezoelectric material with linear feedback, its mechanical response could be characterized by a homogeneous odd elastic material. The external energy exchange favored by the odd elasticity is provided by the modulation of the electric energy. We illustrated these ideas by designing a non-reciprocal Rayleigh wave exhibiting unidirectional invisibility using a homogeneous odd elastic medium and validated them via the equivalent piezoelectric material. The detailed energy gain and release in the odd elastic materials during one loading cycle were also analyzed. Our work offers an easily achievable platform to explore the odd elasticity and interesting phenomena in non-Hermitian systems.

This work was supported by the National Natural Science Foundation of China (Grant Nos. 11632003, 11972083, and 11991030).

1 J. R. Barber, *Elasticity* (Kluwer Academic, Dordrecht, 1992), pp. 117-140.
2 A. E. Green, and P. M. Naghdi, Arch. Rational Mech. Anal. **40**, 37 (1971).
3 D. H. Allen, *How Mechanics Shaped The Modern World* (Springer, Switzerland, 2014), pp. 323-357.
4 S. Ramaswamy, Annu. Rev. Condens. Matter Phys. **1**, 323 (2010), arXiv: 1004.1933.
5 J. Prost, F. Jülicher, and J. F. Joanny, Nat. Phys. **11**, 111 (2015).
6 M. Ravnik, and S. Žumer, Liquid Cryst. **36**, 1201 (2009).
7 M. C. Marchetti, J. F. Joanny, S. Ramaswamy, T. B. Liverpool, J. Prost, M. Rao, and R. A. Simha, Rev. Mod. Phys. **85**, 1143 (2013).
8 G. Gompper, R. G. Winkler, T. Speck, A. Solon, C. Nardini, F. Peruani, H. Löwen, R. Golestanian, U. B. Kaupp, L. Alvarez, T. Kiørboe, E. Lauga, W. C. K. Poon, A. DeSimone, S. Muiños-Landin, A. Fischer, N. A. Söker, F. Cichos, R. Kapral, P. Gaspard, M. Ripoll, F. Sagues, A. Doostmohammadi, J. M. Yeomans, I. S. Aranson, C. Bechinger, H. Stark, C. K. Hemelrijk, F. J. Nedelec, T. Sarkar, T. Aryaksama, M. Lacroix, G. Duclos, V. Yashunsky, P. Silberzan, M. Arroyo, and S. Kale, J. Phys.-Condens. Matter **32**, 193001 (2020), arXiv: 1912.06710.
9 S. Ramaswamy, J. Stat. Mech. **2017(5)**, 054002 (2017), arXiv: 1705.06269.
10 M. Brandenbourger, X. Locsin, E. Lerner, and C. Coulais, Nat. Commun. **10**, 1 (2019), arXiv: 1903.03807.
11 Y. Zhao, X. Zhou, and G. Huang, J. Mech. Phys. Solids **143**, 104065 (2020).
12 R. El-Ganainy, K. G. Makris, M. Khajavikhan, Z. H. Musslimani, S. Rotter, and D. N. Christodoulides, Nat. Phys. **14**, 11 (2018).
13 C. Truesdell, and W. Noll, *The Non-linear Field Theories of Mechanics* (Springer, Berlin, 1965), pp. 117-171.
14 C. Scheibner, A. Souslov, D. Banerjee, P. Surówka, W. T. M. Irvine, and V. Vitelli, Nat. Phys. **16**, 475 (2020), arXiv: 1902.07760.
15 C. Scheibner, W. T. M. Irvine, and V. Vitelli, Phys. Rev. Lett. **125**, 118001 (2020), arXiv: 2001.04969.
16 D. Zhou, and J. Zhang, Phys. Rev. A. **2**, 023173 (2020).
17 V. Soni, E. S. Bililign, S. Magkiriadou, S. Sacanna, D. Bartolo, M. J. Shelley, and W. T. M. Irvine, Nat. Phys. **15**, 1188 (2019).
18 Y. Chen, X. Li, C. Scheibner, G. L. Huang, and V. Vitelli, arXiv: 200907329.
19 J. E. Avron, J. Statist. Phys. **92**, 543 (1997).
20 H. K. Zhang, Y. Chen, X. N. Liu, and G. K. Hu, J. Mech. Phys. Solids **135**, 103796 (2020), arXiv: 1909.09039.
21 H. Nassar, Y. Y. Chen, and G. L. Huang, Proc. Math. Phys. Eng. Sci. **474**, 20180523 (2018).
22 M. Brun, S. Guenneau, and A. B. Movchan, Appl. Phys. Lett. **94**, 061903 (2009), arXiv: 0812.0912.
23 Z. Chang, D. Guo, X. Q. Feng, and G. Hu, Wave Motion **51**, 1170 (2014).
24 L. Rayleigh, Proc. London Math. Soc. **1**, 4 (1885).
25 G. Nolet, *Seismic Wave Propagation and Seismic Tomography* (Springer, Dordrecht, 1987), pp. 1-23.
26 N. Krstulovic-Opara, R. D. Woods, and N. Al-Shayea, Materials **93**, 75 (1996).
27 A. Palermo, P. Celli, B. Yousefzadeh, C. Daraio, and A. Marzani, J. Mech. Phys. Solids **145**, 104181 (2020), arXiv: 2007.10531.
28 Q. Wu, H. Chen, H. Nassar, and G. Huang, J. Mech. Phys. Solids **146**, 104196 (2021).
29 X. M. Zhou, and Y. C. Zhao, Sci. China-Phys. Mech. Astron. **62**, 014612 (2019).
30 A. N. Stroh, J. Math. Phys. **41**, 77 (1962).
31 Y. B. Fu, and A. Mielke, Proc. R. Soc. Lond. A **458**, 2523 (2002).
32 D. F. Parker, Proc. Math. Phys. Eng. Sci. **469**, 20130301 (2013).
33 A. Regensburger, C. Bersch, M. A. Miri, G. Onishchukov, D. N. Christodoulides, and U. Peschel, Nature **488**, 167 (2012).
34 R. Fleury, D. L. Sounas, and A. Alù, Phys. Rev. Lett. **113**, 023903 (2014).

Appendix Stroh formalism for odd elasticity

The main ingredients of Stroh formalism are summarized here, the details can be found in refs. [11,32]. To solve the eigenvalue problem of eq. (14), Stroh formalism is utilized. To proceed, we define

$$\mathbf{Q} = K_{\mathrm{i}1k1} - \rho\delta_{ik}v^2,\ \mathbf{R}_1 = K_{\mathrm{i}1k2},\quad \mathbf{R}_2 = K_{\mathrm{i}2k1},\ \mathbf{S} = K_{\mathrm{i}2k2}. \tag{a1}$$

The normal traction vector $T_i = \sigma_{ij} n_j$ can be written as:

$$\mathbf{T} = -\mathrm{i}p(\mathbf{R}_2 + q\mathbf{S})\mathbf{U} = -\mathrm{i}p\mathbf{I}. \tag{a2}$$

$\mathbf{I}$ is a new traction vector, defined as:

$$q\mathbf{I} = \left(q\mathbf{R}_2 + q^2\mathbf{S}\right)\mathbf{U}. \tag{a3}$$

Using eq. (14), eq. (a3) can be rewritten as:

$$q\mathbf{I} = \left(-\mathbf{Q} + \mathbf{R}_1\mathbf{S}^{-1}\mathbf{R}_2\right)\mathbf{U} - \mathbf{R}_1\mathbf{S}^{-1}\mathbf{I}. \tag{a4}$$

Combining eqs. (a3) and (a4), we get the equation for a generalized eigenvalue problem:

$$\begin{bmatrix} -\mathbf{Q} + \mathbf{R}_1\mathbf{S}^{-1}\mathbf{R}_2 & -\mathbf{R}_1\mathbf{S}^{-1} \\ -\mathbf{S}^{-1}\mathbf{R}_2 & \mathbf{S}^{-1} \end{bmatrix} \begin{bmatrix} \mathbf{U} \\ \mathbf{I} \end{bmatrix} = q \begin{bmatrix} \mathbf{U} \\ \mathbf{I} \end{bmatrix}. \tag{a5}$$

The eigenvalue q must satisfy the following balanced equation:

$$\mathrm{Det}\left[\mathbf{Q} + q(\mathbf{R}_1 + \mathbf{R}_2) + q^2\mathbf{S}\right] = 0. \tag{a6}$$

Then taking the conjugate transpose (denoted by H) on eq. (a6) (where * means conjugate), we obtain

$$\mathrm{Det}\left[\mathbf{Q}^H + q^*\left(\mathbf{R}_1{}^H + \mathbf{R}_2{}^H\right) + (q^*)^2\mathbf{S}^H\right] = 0. \tag{a7}$$

If we take the odd parameters as $\arg(K_0)=\pi/2$, $\mathbf{Q}$, $\mathbf{R}_1+\mathbf{R}_2$, and $\mathbf{S}$ must be of Hermitian matrices, we have

$$\mathrm{Det}\left[\mathbf{Q} + q^*(\mathbf{R}_1 + \mathbf{R}_2) + (q^*)^2\mathbf{S}\right] = 0. \tag{a8}$$

This equation means that q and q^* are both eigenvalues of the problem, so eq. (a5) must have two conjugate pairs, denoted respectively by $q_1^{\pm}$ and $q_2^{\pm}$ (the superscript represents the sign of the imaginary part), the corresponding eigenvectors $\mathbf{U}_j^{\pm}$ represent displacements and $\mathbf{I}_j^{\pm}$ represent tractions (j=1, 2). With the traction-free condition, we have

$$\mathbf{T} = \begin{cases} -\mathrm{i}p_j^+\mathbf{I}_j^+, & v > 0, \\ -\mathrm{i}p_j^-\mathbf{I}_j^-, & v < 0, \end{cases} \quad j = 1, 2, \tag{a9}$$

which means

$$\begin{aligned} &\mathrm{Det}\left[\mathbf{I}_1^+, \mathbf{I}_2^+\right] = 0, \ v > 0, \\ &\mathrm{Det}\left[\mathbf{I}_1^-, \mathbf{I}_2^-\right] = 0, \ v < 0. \end{aligned} \tag{a10}$$

Therefore, we get the surface wave condition for the odd elastic medium, substituting concrete odd parameters into eq. (a10), we can determine the speeds of the edge wave.